

doi: 10.63360/ipmm.v1.e10

Clinical case/ Case Series

A complementary patch-based histogram analysis for quantifying muscle tissue in ultrasound imaging

Borhan Asadi^{1,2}  0000-0001-7505-7958

Sarkout Abdi³  0009-0005-2627-2113

Luis Pérez-Espallargas^{1,2}  0009-0007-7701-9884

Nouredin Nakhostin Ansari⁴  0000-0003-2742-2273

Diego Lapuente-Hernández^{1,2}  0000-0002-6506-6081

¹Healthy Research Group, Instituto de Investigación Sanitaria (IIS) Aragon, University of Zaragoza, 50009 Zaragoza, Spain.

²Department of Physiatry and Nursing, Faculty of Health Sciences, University of Zaragoza, 50009 Zaragoza, Spain.

³Department of Mathematics, Rasht Branch, Islamic Azad University, Rasht, Iran.

⁴Department of Physiotherapy, School of Rehabilitation, Tehran University of Medical Sciences, Tehran, Iran.

ABSTRACT

Introduction: Ultrasound imaging is widely used for muscle assessment due to its non-invasive nature and real-time imaging capabilities. Histogram-based echotexture analysis has proven to be a valuable tool for quantifying muscle tissue composition using features such as echointensity (EI) and echovariation (EV), especially in neuromuscular and neurological disorders. However, variability in region of interest (ROI) selection and image processing methods can significantly affect the extracted echotexture features. This study presents a novel histogram-based analysis approach to investigate the effects of subdividing a single ROI into different patch sizes for muscle tissue assessment. By focusing on the EI and EV of the gastrocnemius medialis in a stroke patient, this research aims to refine quantitative ultrasound analysis to improve clinical applicability.

Case presentation: One stroke patient was randomly selected from a previously collected dataset to perform a complementary analysis. The initially selected grey-scale ROI was extracted and divided into patches of different sizes (10×10, 20×20, 30×30, 40×40 and 50×50 pixels). The EI and EV of each patch were calculated, and their distributions were analyzed using descriptive statistics and correlation methods.

Results: The EV values for patches of sizes 10×10, 20×20, 30×30, 40×40, and 50×50 were 26.48, 24.58, 20.44, 16.78, and 10.38, respectively, which deviated significantly from the original ROI value of 45.54. In contrast, the EI values remained around 81 across all patch sizes, indicating that varying patch sizes did not affect EI.

Conclusions: Patch-based histogram analysis offers a complementary method for assessing muscle texture in ultrasound. While EI appears to be robust to ROI subdivision, EV shows variability, raising concerns about its reliability when small patches are used. Standardized methods and future research with larger datasets are needed to optimize echotexture analysis and ensure reproducibility in clinical practice.

Keywords: Ultrasonography; Muscle tissue; Echotexture analysis; Histogram; Stroke.

1. Introduction

Ultrasound imaging is a non-invasive, safe, accessible, and cost-effective technique commonly used for assessing muscle structure and function. It is widely utilized across various medical fields, including sports medicine, rehabilitation, and the assessment of neuromuscular disorders⁽¹⁻³⁾. One of its primary advantages is that it provides high-resolution, real-time imaging, enabling the visualization of muscle dynamics and tissue changes⁽⁴⁾. Additionally, ultrasound offers valuable quantitative and qualitative insights into muscle tissue, making it an essential tool for diagnosing and monitoring muscle diseases and alterations⁽⁵⁾. However, despite significant advances in ultrasound technology, the quantitative analysis of ultrasound images remains a major challenge in medical and clinical research.

Image texture is commonly defined as the spatial variation of pixel intensity, and in ultrasound imaging, this concept is referred to as echotexture^(6,7). This definition is widely accepted in image processing, where texture analysis techniques are employed for classification, segmentation, and synthesis⁽⁸⁾. Several computational approaches have been developed to facilitate the identification of complex tissue patterns from texture feature extraction from images, such as the gray-level co-occurrence matrix (GLCM), gray-level run-length matrix (GLRLM), Fast Fourier transform (FFT), and neural networks⁽⁹⁾.

Among these approaches, histogram analysis has received considerable attention due to its simplicity and utility in the assessment of muscle composition, particularly in the evaluation of neuromuscular disorders^(7, 10-12). This technique examines the distribution of pixel intensities within ultrasound images, allowing the extraction of first-order statistical features such as mean, standard deviation, skewness, kurtosis, energy, or entropy⁽¹³⁾. Previous studies have shown that these statistical parameters derived from histogram analysis can characterize muscle tissue quality in different health conditions, demonstrating their potential for use in clinical settings⁽¹⁴⁻¹⁸⁾. The advantage of histogram-based (first-order) parameters over second-order parameters such as GLCM and GLRLM is that they can be directly computed from the original pixel values and the initial image matrix. In contrast, second-order parameters require the prior calculation of GLCM and GLRLM matrices before extracting the desired features. On the other hand, second-order parameters may provide additional texture information that cannot be captured by first-order parameters.

Among the key quantitative features extracted from muscle tissue in neuromuscular disorders and other neurological disorders such as stroke, echointensity (EI) and echovariation (EV) have proven to be particularly relevant and applicable to clinical practice^(12,19-21). On the one hand, EI determines the mean pixel intensity, while EV quantifies the variation of the EI. In particular, a study by Asadi et al.⁽²⁰⁾ analyzed ultrasound images of the gastrocnemius medialis in stroke individuals and found a strong inverse correlation between EV and the modified Heckmatt scale. However, this scale has notable limitations due to its subjective nature and its restricted four-grade grading system⁽²²⁾, so EV was proposed as a reliable quantitative approach to assess muscle tissue quality in individuals with stroke⁽²⁰⁾.

In the aforementioned study⁽²⁰⁾ the region of interest (ROI) for echotexture feature extraction was defined as the largest possible area of muscle tissue between the superficial and deep fascia.

However, there is considerable variability in the selection and size of ROIs among studies analyzing muscle echotexture^(19,23-26). In addition to this variability, when performing the histogram analysis on a selected ROI, it remains unclear to what extent the chosen methodology influences the extracted echotexture features. Some studies may simply select the entire ROI as a single unit, while others may segment the same image into multiple ROIs, or even divide each ROI into patches of different sizes. The previous histogram-based analyses often considered one ROI without accounting for spatial heterogeneity within the muscle⁽¹⁴⁻¹⁸⁾. This limitation may lead to an oversimplified representation of muscle echotexture, potentially missing localized pathological changes. The proposed patch-based analysis methodology could provide a more complete and reliable representation of the selected ROI, as it generates a distribution of values rather than a single value and may also enhance sensitivity to subtle tissue alterations. However, the impact of this approach on key muscle tissue analysis features, such as EI and EV, is unknown.

Therefore, the primary objective of this study was to perform a complementary analysis of EI and EV variations in a single stroke patient using a histogram-based analysis by dividing the original ROI into patches of different sizes. This study aims to investigate whether patch-based division influences histogram-derived muscle tissue analysis, specifically examining the impact of patch size on the assessment of echotexture in ultrasound images.

2. Description of the clinical case

2.1 Patient information

A single participant was selected from the study's dataset by Asadi et al.⁽²⁰⁾. This stroke patient was recruited from the Hospital Clínico Universitario Lozano Blesa in April 2024. Inclusion criteria required participants to be older than 18 years, have a confirmed diagnosis of stroke verified by computed tomography (CT) or magnetic resonance imaging (MRI), and be able to walk independently, with or without assistance. Exclusion criteria included the presence of other neurological disorders, history of lower extremity surgery, or any medical condition that could interfere with data collection. The study was approved by the Aragon Ethics Committee (PI24/030) and registered in ClinicalTrials.gov (NTC06411587). In addition, the study adhered to the ethical guidelines of the Declaration of Helsinki⁽²⁷⁾.

2.2 Data Collection

In the study by Asadi et al.⁽²⁰⁾, ultrasound images were acquired using the Butterfly iQ+ portable ultrasound system, following a standardized imaging protocol with a gain setting of 50% and a depth setting of 5-7 cm. A trained physiotherapist performed the scans while the patients were seated with knees flexed at 90°. The ultrasound probe was placed proximally at 30% of the distance between the medial condyle of the tibia and the medial malleolus, with an adjusted angle of approximately 35-45° to optimize image quality.

For this case study, a single image of the gastrocnemius medialis muscle was randomly selected from the data set collected by Asadi et al.⁽²⁰⁾ for detailed analysis. The method of muscle tissue extraction was identical to that used in the original study, and this extracted area was considered the main ROI, carefully chosen to include as much muscle tissue as possible while

excluding superficial and deep fascia⁽²⁸⁾. The selected original ROI was then converted from color to grayscale using a Python-based program for further analysis.

2.3 Data Analysis

In this case study, the grayscale ultrasound ROI was divided into square patches of predefined sizes (10×10, 20×20, 30×30, 40×40, and 50×50 pixels). Each patch size is shown in Figures 1 to 5 of the supplementary material. For each patch, EI, defined as the mean intensity of the pixels within the ROI, and EV, defined as the ratio of the standard deviation to the mean intensity, were calculated. The corresponding formulae are as follows:

$$\frac{1}{N} \sum_{i=1}^N x_i \quad \text{for EI} \qquad \frac{\sum_{i=1}^N (x_i - \mu)^2}{\sum_{i=1}^N x_i} \quad \text{for EV}$$

Descriptive statistics were calculated to characterize the EI and EV value distribution, including mean, standard deviation, median, interquartile range (IQR), and skewness. Skewness was used to classify the shape of the distribution as normal, right-skewed, or left-skewed. Histograms of both features were generated to visualize their distributions, with annotations highlighting key statistical measures.

The normality of the EI and EV distributions was first assessed by inspecting the histograms. If the distribution appeared normal, the mean and standard deviation were used for further analysis; whereas if the distribution of EI or EV was skewed (right or left), the median and IQR were used instead. In both cases, the correlation between EI or EV and data dispersion was calculated using Kendall's tau coefficient, a rank-based method well suited for small data sets^(29,30).

The selected statistical measures were then compared with the original EI and EV values of the original ROI in a graphical representation to evaluate the observed changes and assess the dispersion of EV and EI depending on the patch size selected for the ROI. Additionally, to improve visualization and facilitate a clearer and more accurate comparison of variations, changes in EV were scored on the primary EV function for stroke patients derived from the study by Asadi et al.⁽²⁰⁾. This function showed that higher EV values were associated with better muscle tissue quality, whereas lower EV values correspond to greater muscle impairment in stroke-affected muscles⁽²⁰⁾. Therefore, the mean or median EV values extracted from the histograms were plotted on the function: $y = a \cdot e^{bx} + c \cdot e^{dx} + E$; using the parameters: $a = 37.13$, $b = -0.14$, $c = 132,052.16$, $d = -2 \cdot 10^{-6}$, and $E = -131,990.30$. There is no equivalent function for EI, which precludes applying the same approach to this feature.

3. Results

The distribution type, mean, standard deviation, median, and IQR were calculated for the original ROI with five different patch sizes: 10×10, 20×20, 30×30, 40×40, and 50×50 pixels. The results indicated that the histogram showed a normal distribution for the EI feature, whereas the EV feature showed a right-skewed distribution, suggesting that the EV data did not conform to normality. Figure 1 presents the histogram plots for EI, while Figure 2 shows the histogram plots for EV for each patch size.

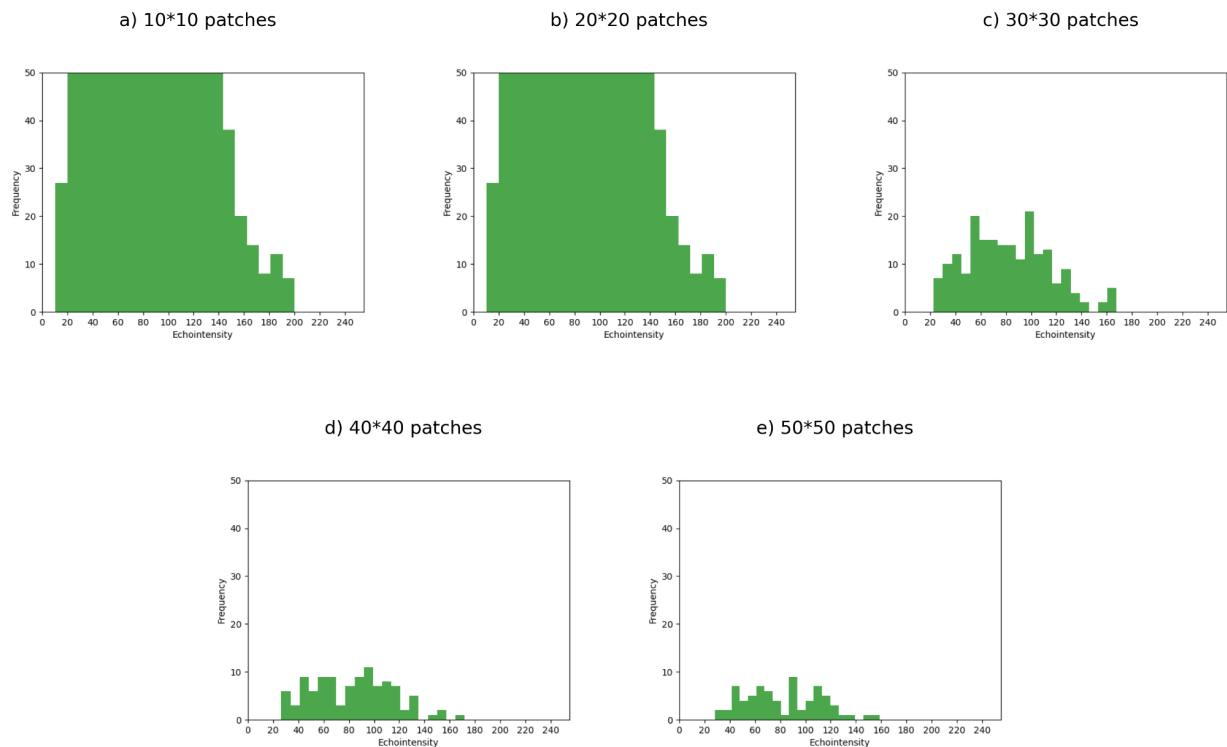


Figure 1. Echointensity histograms derived from the original ROI of the ultrasound image of the gastrocnemius medialis muscle. The x-axis represents the echointensity values, while the y-axis indicates the frequency of occurrence. (a) Histogram for 10×10 pixel patches, (b) 20×20 pixel patches, (c) 30×30 pixel patches, (d) 40×40 pixel patches and (e) 50×50 pixel patches.

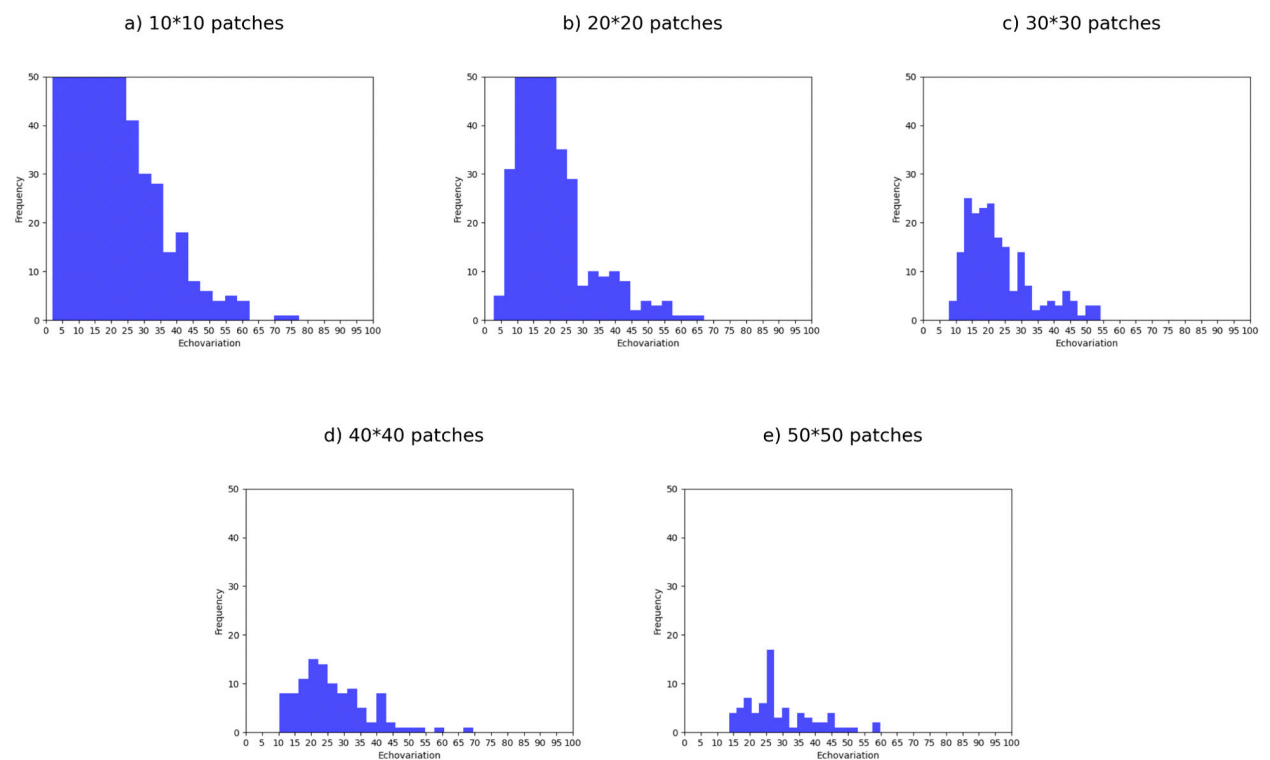


Figure 2. Echovariation histograms derived from the original ROI of the ultrasound image of the gastrocnemius medialis muscle. The x-axis represents the echovariation values, while the y-axis indicates the frequency of occurrence. (a) Histogram for 10×10 pixel patches, (b) 20×20 pixel patches, (c) 30×30 pixel patches, (d) 40×40 pixel patches and (e) 50×50 pixel patches.

On the one hand, since the EI values followed a normal distribution, the mean and standard deviation were used to describe the data. Kendall's correlation coefficient yielded a value of -0.4, indicating no significant correlation between the mean EI and its standard deviation. Figure 3 illustrates the EI and standard deviation variations for each patch size. Both parameters remained relatively stable across the different patches, with values approaching the 81.89 value of the EI of the original ROI.

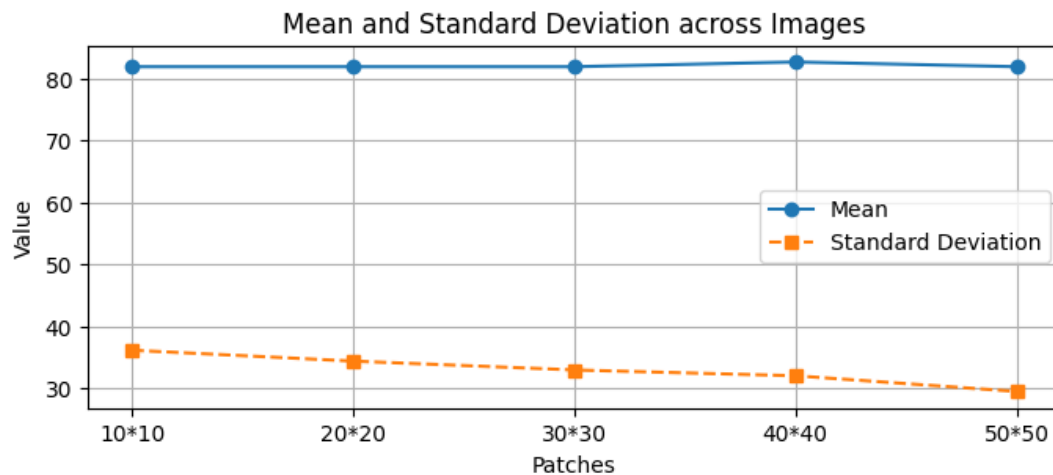


Figure 3. Line graph illustrating the mean and standard deviation values of echointensity for each patch size. The X-axis represents the patch sizes, while the Y-axis indicates the corresponding values of the mean and standard deviation of echointensity. The blue line represents the mean and the orange line the standard deviation.

On the other hand, the EV values followed a non-normal distribution, which made it necessary to use the median and IQR to summarize the data. In addition, Kendall's correlation coefficient yielded a value of 1, indicating a perfect correlation between median EV and IQR values. Figure 4 illustrates the variations of median EV and IQR in the histograms for the predefined patch sizes. The highest median EV value (26.48) was observed at the 50×50 patch size, which was still substantially lower than the EV value of 45.54 of the original ROI. In addition, the dispersion values indicate that smaller patch sizes showed the lowest IQR, while larger patch sizes showed an increasing IQR (Figure 4). Therefore, as the patch size increases, both the dispersion and the median EV increase, progressively approximating the EV value of the original ROI.



Figure 4. Line graph illustrating the median and interquartile range (IQR) values of echovariation for each patch size. The X-axis represents the patch sizes, while the Y-axis indicates the corresponding values of the median and IQR of echovariation. The blue line represents the median and the orange line the IQR.

The median EV values extracted from the histograms were plotted on the function derived from the study by Asadi et al.⁽²⁰⁾ In our case study, the results revealed a clear trend: as patch size decreased, median EV shifted toward values characteristic of more affected regions; conversely, as patch size increased, median EV approached the EV value of the original ROI (Figure 5).

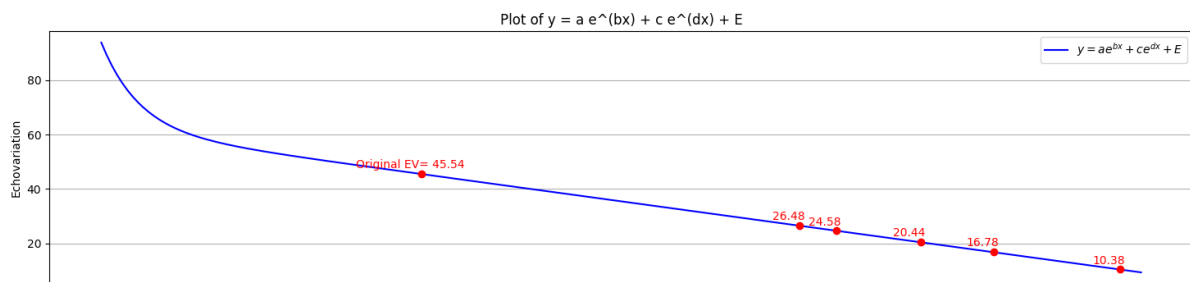


Figure 5. Visualization of the median values of echovariation (EV) extracted from the histograms for different patch sizes, represented in the function of the study by Asadi et al. (20). From left to right: 45.54 represents the original ROI, 26.48 corresponds to the 50×50 patch, 24.58 to the 40×40, 20.44 to the 30×30, 16.78 to the 20×20, and 10.38 to the 10×10 pixel.

4. Discussion

Numerous studies have employed histogram-based approaches to extract quantitative features from ultrasound images. Some researchers have refined this methodology by segmenting the image in different ROIs before applying histogram analysis to improve diagnostic accuracy and interpretability^(31, 32). This segmentation-based approach allows a localized assessment of tissue features, which is particularly valuable in medical imaging. To our knowledge, no previous studies have explored whether dividing the ROI into patches produces different results than analyzing the entire ROI, which remains the most commonly used method in histogram-based analysis. Furthermore, to our knowledge and our findings, no research has examined how patch size influences histogram-derived outcomes when applying a patch-based approach. The proposed methodology could provide a more representative characterization of muscle tissue and improve the reliability of comparisons between studies with similar objectives.

In this study, we integrate histogram-based analysis with a patch-based dividing strategy of the ROI, which included the maximal amount of muscle tissue in the gastrocnemius medialis. Our results indicate that mean EI values calculated from patches accurately reflect the EI of the original ROI. In contrast, the median EV values obtained from patches do not reliably represent the EV of the original ROI. This discrepancy is critical, as previous research has successfully classified muscle tissue characteristics in stroke patients based on EV values⁽²⁰⁾. If the EV values of smaller patches deviate significantly from the actual EV of the original ROI, questions arise about the reliability of using the mean EV values of patches for clinical or diagnostic purposes. Our results suggest that relying on the median EV of smaller patches could lead to misinterpretations, as these values may not accurately reflect the severity of muscle impairment⁽²⁰⁾.

Regarding the standard deviation or IQR values, our analysis demonstrates that, for the EI feature, there are no differences in the standard deviation values extracted from the patched ROI compared to the original ROI. However, for the EV feature, there is a systematic increase in the IQR as the patch size increases. This finding is crucial, as it suggests that changes in patch size

influence the statistical representation and, consequently, the interpretation of EV on ultrasound images, which has been defined as a relevant ultrasonographic objective indicator in previous studies for different neurological populations^(19,20). Consistent with our findings, several previous studies have explored how different methods of segmenting ROIs within the same ultrasound image may affect, for example, the performance of automated tumor selection algorithms⁽³³⁾ or luminal contour detection in intravascular ultrasound⁽³⁴⁾.

A limitation of our study is that the analysis was performed on a single ultrasound image and only analyzed in a ROI size, which included the maximal amount of muscle tissue. Although the results of this methodology suggest a clear pattern and indicate that the EI feature can be used reliably, unlike EV, further studies are needed to validate these findings. Future research should include comparisons using more images for each patch size and assess the impact of different ROI sizes within the same image. In addition, it is essential to investigate whether a standardized patch division strategy across an entire dataset could improve the classification of ultrasound images by correlating the results with validated tools such as the Heckmatt scale. A uniform approach could allow for more consistent feature extraction and improve differentiation between healthy and affected tissues. These studies are crucial to determine whether this methodological framework could improve the diagnostic value of echotexture analysis, particularly for the EV feature.

5. Conclusion

This study explored a complementary patch-based histogram analysis to assess muscle tissue characteristics in ultrasound images, focusing on EI and EV features. Our findings indicate that the EI values from divided patches closely align with the original ROI's, supporting their stability as a valuable muscle tissue characterization indicator. However, EV values from smaller patches deviate significantly from the original ROI, raising questions about its reliability for clinical applications, as the variations in ROI division influence its statistical representation. Although this study is limited to a single ultrasound image in a single ROI size, the results underscore the need for standardized methodologies in histogram-based analysis and further research to refine the use of EV in diagnostic applications of ultrasound imaging.

References

1. Whittaker JL, Stokes M. Ultrasound imaging and muscle function. *J Orthop Sports Phys Ther.* 2011;41(8):572–80. doi:10.2519/jospt.2011.3682
2. Chang KV, Wu WT, Özçakar L. Ultrasound imaging and rehabilitation of muscle disorders: part 1. Traumatic injuries. *Am J Phys Med Rehabil.* 2019;98(12):1133–41. doi:10.1097/PHM.0000000000001307
3. Hodges PW. Ultrasound imaging in rehabilitation: just a fad? *J Orthop Sports Phys Ther.* 2005;35(6):333–7. doi:10.2519/jospt.2005.0106
4. Stokes M, Hides J, Nassiri DK. Musculoskeletal ultrasound imaging: diagnostic and treatment aid in rehabilitation. *Phys Ther Rev.* 1997;2(2):73–92. doi: 10.1179/ptr.1997.2.2.73
5. Naruse M, Trappe S, Trappe TA. Human skeletal muscle size with ultrasound imaging: a comprehensive review. *J Appl Physiol (1985).* 2022;132(5):1267–79. doi:10.1152/jappphysiol.00041.2022

6. Materka A, Strzelecki M. Texture Analysis Methods - A Review. Technical University of Lodz, Institute of Electronics, COST B11 Report. 1998.
7. Paris MT, Mourtzakis M. Muscle composition analysis of ultrasound images: a narrative review of texture analysis. *Ultrasound Med Biol*. 2021;47(4):880–95. doi:10.1016/j.ultrasmedbio.2020.12.012
8. Nailon WH. Texture analysis methods for medical image characterisation. *Biomed Imaging*. 2010;75:100. doi:10.5772/8912
9. Lubner MG, Smith AD, Sandrasegaran K, Sahani DV, Pickhardt PJ. CT texture analysis: definitions, applications, biologic correlates, and challenges. *Radiographics*. 2017;37(5):1483–503. doi:10.1148/rgr.2017170056
10. Mailloux GE, Bertrand M, Stampfler R, Ethier S. Local histogram information content of ultrasound B-mode echographic texture. *Ultrasound Med Biol*. 1985;11(5):743–50. doi:10.1016/0301-5629(85)90108-5
11. Pillen S, Van Alfen N. Muscle ultrasound from diagnostic tool to outcome measure—Quantification is the challenge. *Muscle Nerve*. 2015;52(3):319–20. doi:10.1002/mus.24613
12. Pillen S, Arts IM, Zwarts MJ. Muscle ultrasound in neuromuscular disorders. *Muscle Nerve*. 2008;37(6):679–93. doi:10.1002/mus.21015
13. Shannon CE. A mathematical theory of communication. *ACM SIGMOBILE Mob Comput Commun Rev*. 2001;5(1):3–55. doi:10.1145/584091.584093
14. Sogawa K, Nodera H, Takamatsu N, Mori A, Yamazaki H, Shimatani Y, et al. Neurogenic and myogenic diseases: quantitative texture analysis of muscle US data for differentiation. *Radiology*. 2017;283(2):492–8. doi:10.1148/radiol.2016160826
15. Ismail C, Zabal J, Hernandez HJ, Woletz P, Manning H, Teixeira C, et al. Diagnostic ultrasound estimates of muscle mass and muscle quality discriminate between women with and without sarcopenia. *Front Physiol*. 2015;6:302. doi:10.3389/fphys.2015.00302
16. Pagán-Conesa A, García-Ortiz MT, Salmerón-Martínez EJ, Moya-Martínez A, López-Prats F. Diagnostic ultrasound shows reversal of supraspinatus muscle atrophy following arthroscopic rotator cuff repair. *Arthroscopy*. 2021;37(10):3039–48. doi:10.1016/j.arthro.2021.04.039
17. Harris-Love MO, Gonzales TI, Wei Q, Ismail C, Zabal J, Woletz P, et al. Association between muscle strength and modeling estimates of muscle tissue heterogeneity in young and old adults. *J Ultrasound Med*. 2019;38(7):1757–68. doi:10.1002/jum.14864
18. Calvo-Lobo C, Useros-Olmo AI, Almazán-Polo J, Martín-Sevilla M, Romero-Morales C, Sanz-Corbalán I, et al. Quantitative ultrasound imaging pixel analysis of the intrinsic plantar muscle tissue between hemiparesis and contralateral feet in post-stroke patients. *Int J Environ Res Public Health*. 2018;15(11):2519. doi:10.3390/ijerph15112519
19. Martínez-Payá JJ, Ríos-Díaz J, Del Baño-Aledo ME, Tembl-Ferrairó JI, Vazquez-Costa JF, Medina-Mirapeix F. Quantitative muscle ultrasonography using textural analysis in amyotrophic lateral sclerosis. *Ultrason Imaging*. 2017;39(6):357–68. doi:10.1177/0161734617711370
20. Asadi B, Pujol-Fuentes C, Carcasona-Otal A, Calvo S, Herrero P, Lapuente-Hernández D. Characterizing muscle tissue quality post-stroke: echovariation as a clinical indicator. *J Clin Med*. 2024;13(24). doi:10.3390/jcm13247800

21. Akazawa N, Harada K, Okawa N, Kishi M, Tamura K, Moriyama H. Changes in quadriceps thickness and echo intensity in chronic stroke survivors: a 3-year longitudinal study. *J Stroke Cerebrovasc Dis.* 2021;30(3):105543. doi: [10.1016/j.jstrokecerebrovasdis.2020.105543](https://doi.org/10.1016/j.jstrokecerebrovasdis.2020.105543)
22. Heckmatt JZ, Leeman S, Dubowitz V. Ultrasound imaging in the diagnosis of muscle disease. *J Pediatr.* 1982;101(5):656–60. doi: [10.1016/s0022-3476\(82\)80286-2](https://doi.org/10.1016/s0022-3476(82)80286-2)
23. Molinari F, Caresio C, Acharya UR, Mookiah MR, Minetto MA. Advances in quantitative muscle ultrasonography using texture analysis of ultrasound images. *Ultrasound Med Biol.* 2015;41(9):2520–32. doi: [10.1016/j.ultrasmedbio.2015.04.021](https://doi.org/10.1016/j.ultrasmedbio.2015.04.021)
24. Sahinis C, Kellis E. Hamstring muscle quality properties using texture analysis of ultrasound images. *Ultrasound Med Biol.* 2023;49(2):431–40. doi: [10.1016/j.ultrasmedbio.2022.09.011](https://doi.org/10.1016/j.ultrasmedbio.2022.09.011)
25. Escriche-Escuder A, Trinidad-Fernández M, Pajares B, Iglesias-Campos M, Alba E, García-Almeida JM, et al. Responsiveness of the new index muscular echotexture in women with metastatic breast cancer: an exercise intervention study. *Sci Rep.* 2022;12(1):15148. doi: [10.1038/s41598-022-19532-7](https://doi.org/10.1038/s41598-022-19532-7)
26. Del-Canto-Fernández A, Calleja-Martínez P, Descalzo-Hoyas B, Rodríguez-Posada S, Cuenca-Zaldívar N, Fernández-Carnero S, et al. The application of image texture analysis techniques on the effects of dry needling versus placebo in low-back pain patients: a pilot study. *Appl Sci.* 2022;12(11):5556. doi: [10.3390/app12115556](https://doi.org/10.3390/app12115556)
27. Shrestha B, Dunn L. The declaration of Helsinki on medical research involving human subjects: a review of seventh revision. *J Nepal Health Res Coun.* 2020;17(4):548–52. doi: [10.33314/jnhrc.v17i4.1042](https://doi.org/10.33314/jnhrc.v17i4.1042)
28. Caresio C, Molinari F, Emanuel G, Minetto MA. Muscle echo intensity: reliability and conditioning factors. *Clin Physiol Funct Imaging.* 2015;35(5):393–403. doi: [10.1111/cpf.12175](https://doi.org/10.1111/cpf.12175)
29. Bujang MA. An elaboration on sample size determination for correlations based on effect sizes and confidence interval width: a guide for researchers. *Restor Dent Endod.* 2024;49(2):e21. doi: [10.5395/rde.2024.49.e21](https://doi.org/10.5395/rde.2024.49.e21)
30. Hunsberger S, Long L, Reese SE, Hong GH, Myles IA, Zerbe CS, et al. Rank correlation inferences for clustered data with small sample size. *Stat Neerl.* 2022;76(3):309–30. doi: [10.1111/stan.12261](https://doi.org/10.1111/stan.12261)
31. Kermani A, Ayatollahi A, Talebi M. Segmentation of medical ultrasound image based on local histogram range image. In: 3rd International Conference on Biomedical Engineering and Informatics; 2010. IEEE. doi: [10.1109/BMEI.2010.5639996](https://doi.org/10.1109/BMEI.2010.5639996)
32. Zhu Q. Ultrasonic image analysis of cardiac space-occupying diseases based on grey clustering algorithm. In: 2023 International Conference on Telecommunications, Electronics and Informatics (ICTEI); 2023. IEEE. doi: [10.1109/ICTEI60496.2023.00173](https://doi.org/10.1109/ICTEI60496.2023.00173)
33. Zhang D, Liu Y, Yang Y, Xu M, Yan Y, Qin Q. A region-based segmentation method for ultrasound images in HIFU therapy. *Med Phys.* 2016;43(6):2975–89. doi: [10.1118/1.4950706](https://doi.org/10.1118/1.4950706)
34. Dos Santos E, Yoshizawa M, Tanaka A, Saijo Y, Iwamoto T. Detection of luminal contour using fuzzy clustering and mathematical morphology in intravascular ultrasound images. *Conf Proc IEEE Eng Med Biol Soc.* 2005;2005:3471–4. doi: [10.1109/iembs.2005.1617226](https://doi.org/10.1109/iembs.2005.1617226)

Supplementary material

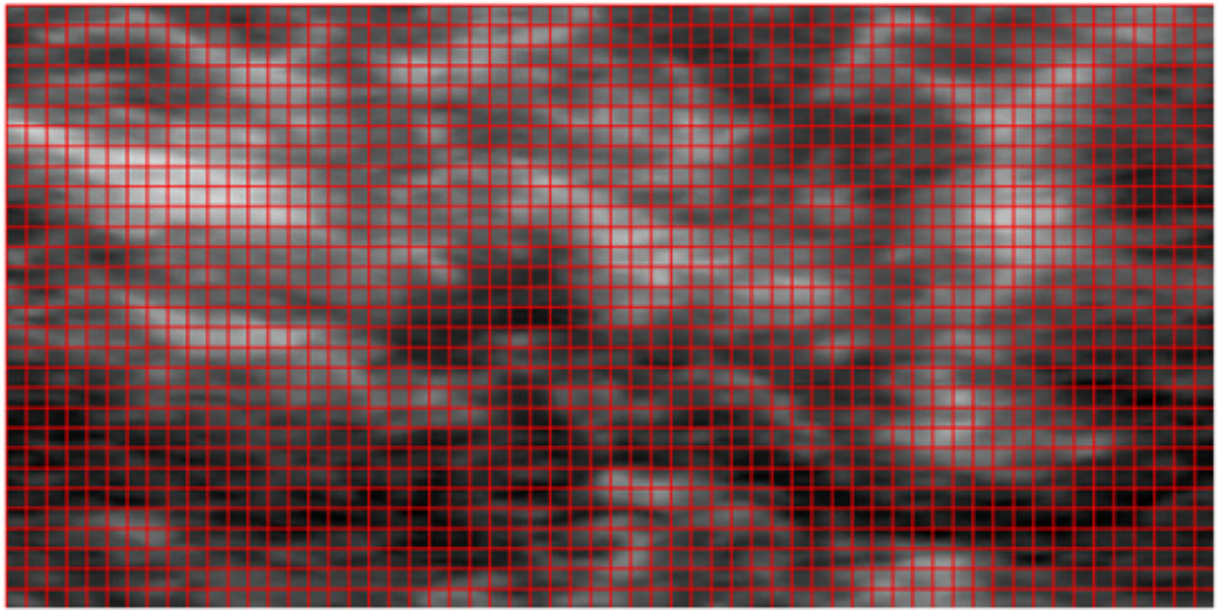


Figure S1. Original ROI of the whole muscle segmented into 10*10 pixel patches.

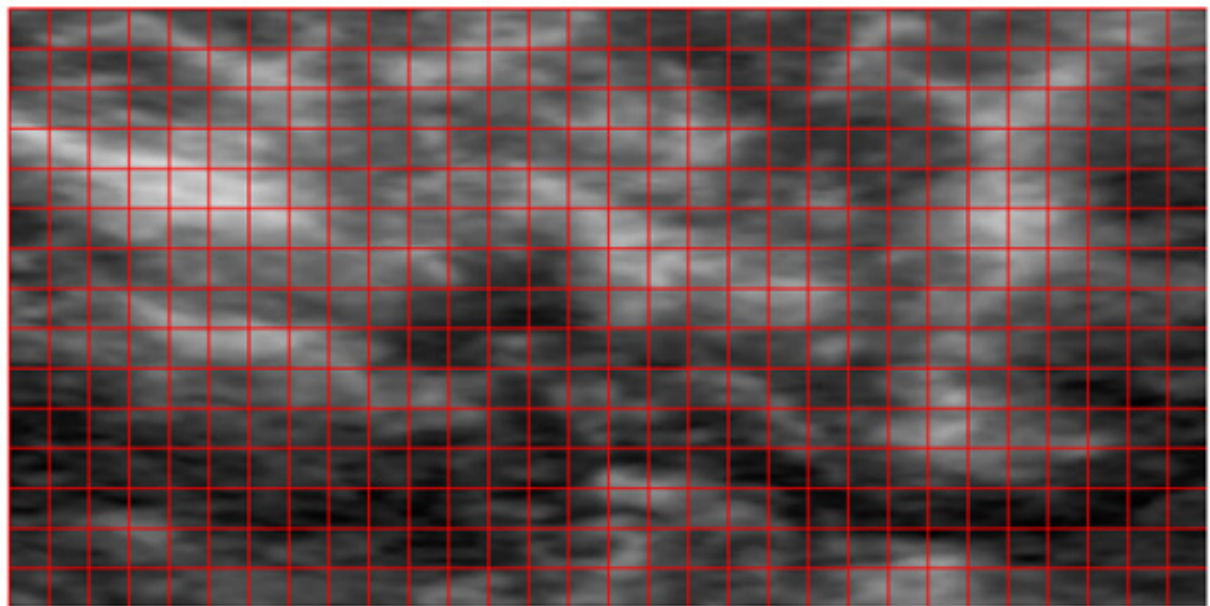


Figure S2. Original ROI of the whole muscle segmented into 20*20 pixel patches.

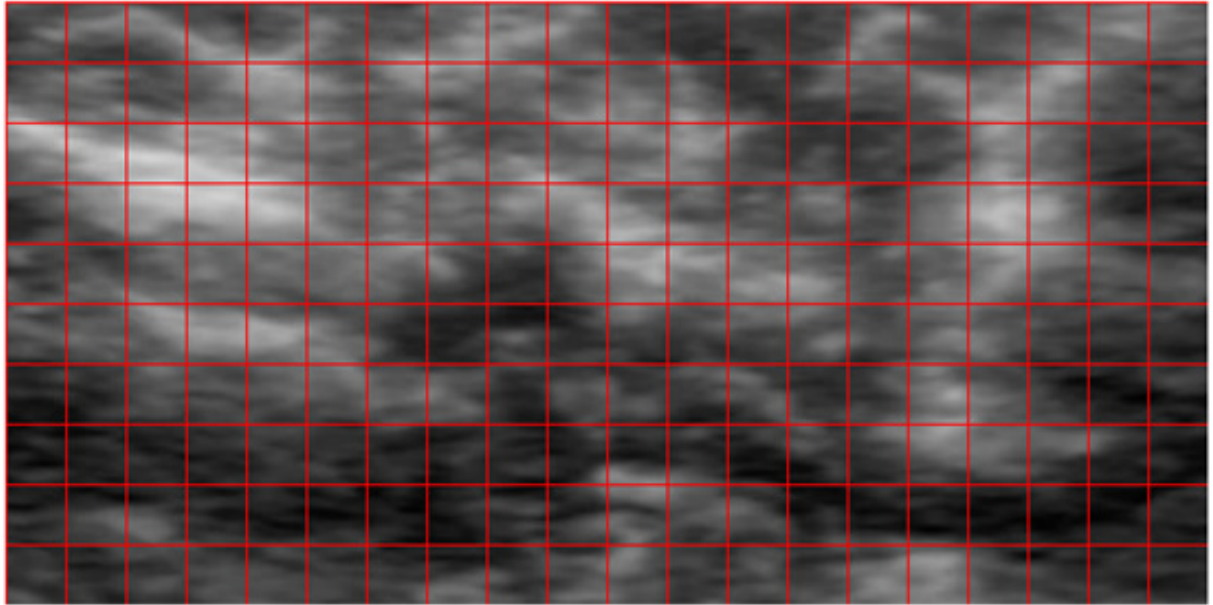


Figure S3. Original ROI of the whole muscle segmented into 30*30 pixel patches.

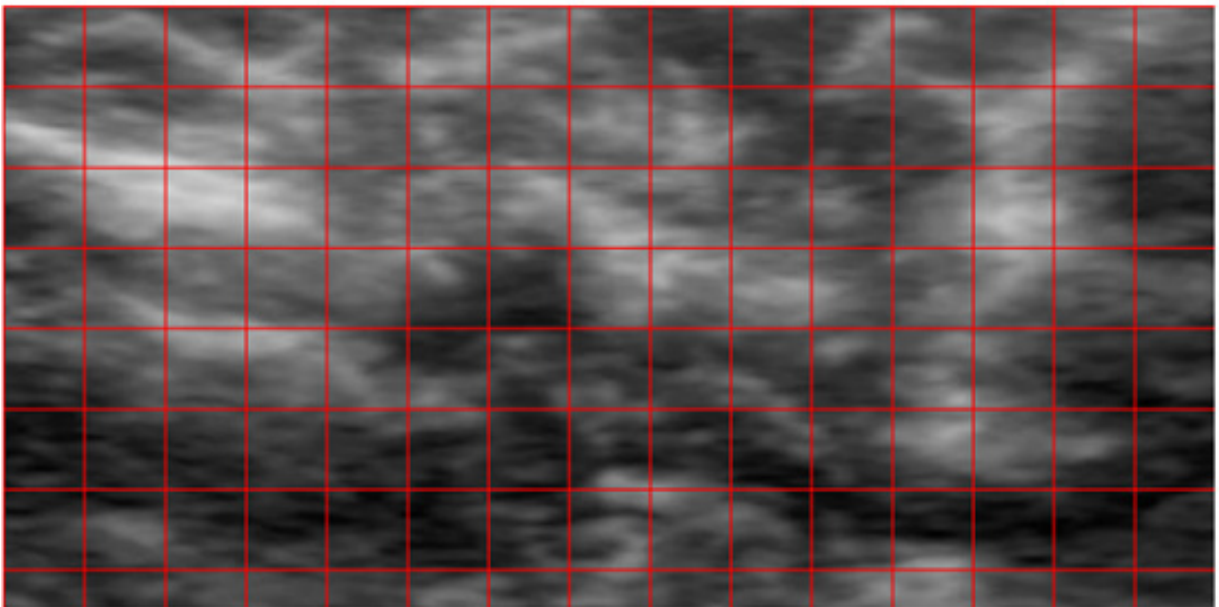


Figure S4. Original ROI of the whole muscle segmented into 40*40 pixel patches.

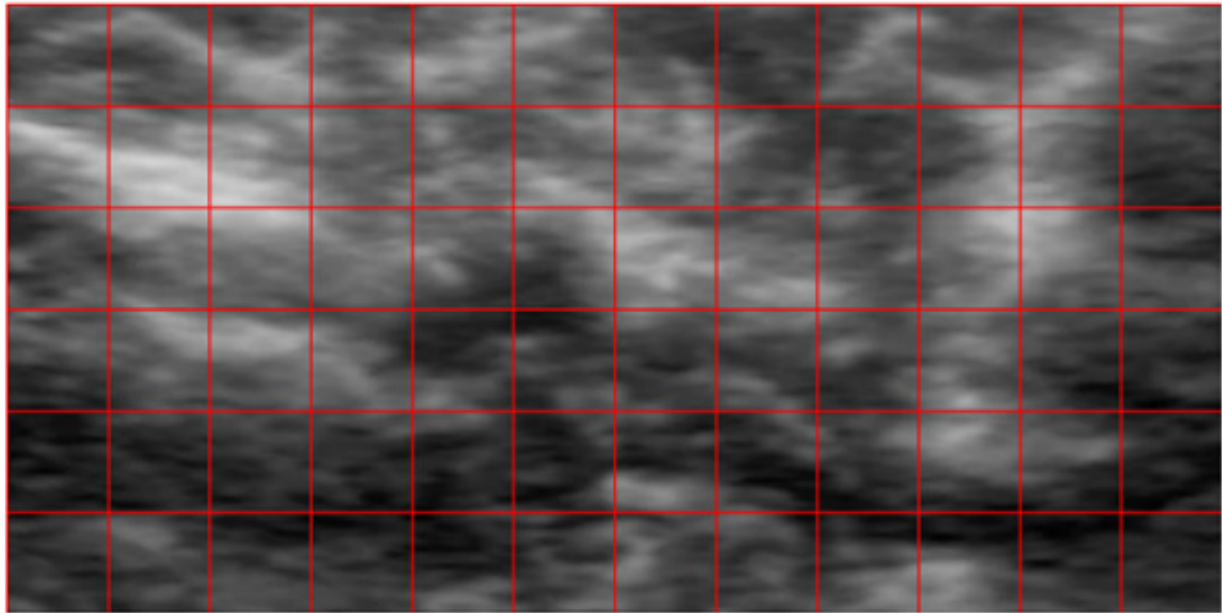


Figure S5. Original ROI of the whole muscle segmented into 50*50 pixel patches.

Editorial information

✉ Correspondence

basadi@iisaragon.es

Dates

Received: 16.03.2025

Accepted: 12.04.2025

Published: 22.04.2025

Author Contributions

Conceptualization, B.A. and D.L.-H.; methodology, B.A. and D.L.-H.; software, B.A.; validation, D.L.-H.; formal analysis, B.A. and D.L.-H.; investigation, B.A. and D.L.-H.; data curation, B.A.; writing—original draft preparation, B.A. and D.L.-H.; writing—review and editing, B.A., S.A., L.P., N.N.A. and D.L.-H.; visualization, B.A.; supervision, D.L.-H.; project administration, B.A. and D.L.-H.; All authors have read and agreed to the published version of the manuscript.

Funding

This research received no external funding.

Patient's informed consent

Informed consent was obtained from all the subjects involved in this study. Written informed consent was obtained from the patients to publish this paper.

Data Availability Statement

The data presented in this study are available from the corresponding author upon request, due to the fact that these data are part of a larger, ongoing project and may not yet be fully available for public sharing until the project is completed.

Conflicts of Interest

The authors declare no conflicts of interest.

Suggested citation

Asadi B, Abdi S, Pérez-Espallargas L, Nakhostin Ansari N, Lapuente-Hernández D. A complementary patch-based histogram analysis for quantifying muscle tissue in ultrasound imaging. Invasive Physiother Musculoskelet Med. 2025;1:e10. doi: 10.63360/ipmm.v1.e10

Disclaimer/Publisher's Note

The statements, opinions, and data contained in all publications are solely those of the individual author(s) and contributor(s) and not of IPMM and/or the editor(s). IPMM and/or the editor(s) disclaim responsibility for any injury to people or property resulting from any ideas, methods, instructions, or products referred to in the content.

Copyright

© 2025 by the authors.

Publication under the terms and conditions of the Creative Commons Attribution (CC BY-NC-SA) license (<https://creativecommons.org/licenses/by-nc-sa/4.0>)